

Received: 2017.12.05
Accepted: 2018.02.05
Published: 2018.07.12

Partial Recovery of Limb Function Following End-to-Side Screw Anastomosis of Phrenic Nerve in Rats with Brachial Plexus Injury

Authors' Contribution:
Study Design A
Data Collection B
Statistical Analysis C
Data Interpretation D
Manuscript Preparation E
Literature Search F
Funds Collection G

A 1 **Guang-Liang Hao**
B 2 **Tian-Yin Zhang**
C 1 **Qiang Zhang**
D 1 **Ming-Yong Gu**
C 1 **Chen Chen**
B 1 **Lin Zou**
C 1 **Xue-Cheng Cao**
D 1 **Gui-Chun Zhang**

1 Department of Orthopedics, Jinan Military General Hospital, Jinan, Shandong, P.R. China
2 Department of Surgery, First People's Hospital of Jinan, Jinan, Shandong, P.R. China

Corresponding Author: Gui-Chun Zhang, e-mail: zhangguichunzgc@yeah.net
Source of support: Departmental sources

Background: Brachial plexus injury (BPI), a severe nervous system injury, is a leading cause of functional damages of the affected upper limb. Patients with BPI manifested with motor weakness or paralysis, sensory deficits, and pain. We established a BPI rat model to explore the *in vivo* effect of end-to-side screw anastomosis (ETSSA) of phrenic nerve on the recovery of limb function after BPI.





Material/Methods: After modeling, rats were treated with end-to-side anastomosis (ETSA) and ETSSA respectively. After 1 and 3 months, the behavioral changes of rats were observed using the Terzis grooming test, and the compound muscle action potential (CMAP) and muscle tension of biceps brachii were detected. The muscle weight recovery rate (MWRR) and cross-sectional area recovery rate (CARR) were calculated. Toluidine blue staining was used to observe the myelinated nerve fibers in the proximal phrenic nerve and distal musculocutaneous nerve of suture. The ratio of regenerated nerve traversing rate (NTR) was counted and motor endplate area of biceps brachii was measured.

Results: The rats treated with ETSA and ETSSA exhibited elevated grading of Terzis grooming test with time. Although both the ETSSA and ETSA can reduce the MWRR, CARR and motor endplate area in BPI rats, ETSSA showed a better influence on the latency delayed rate (LDR) and amplitude recovery rate (ARR) of CMAP, muscular tension recovery rate (MTRR), MWRR, number of regenerated myelinated nerve fibers, NTR, and motor endplate area in BPI rats.

Conclusions: Our study provided evidence that ETSSA can restore the limb function recovery to a greater extent, and accelerate the regeneration of nerve fibers in rats with BPI; the effect of ETSSA was better than that of ETSA.

MeSH Keywords: **Orthopedics • Phrenic Nerve • Arteriovenous Anastomosis**

Full-text PDF: <https://www.medscimonit.com/abstract/index/idArt/908379>

 3849  4  6  24



Background

Brachial plexus injury (BPI), as a severe neurologic injury, is caused by severe traction force on the upper limb, leading to complete or partial motor paralysis [1]. There are several factors responsible for BPI such as gestational diabetes mellitus, neonatal macrosomia, vaginal delivery, breech presentation, and shoulder dystocia [2]. Although the majority of BPI cases can resolve spontaneously within a year, approximately 5% to 8% cases will still, persist which is a leading cause of birth related litigation [3]. The treatment for BPI relies on the pathologic condition and the position of the injury [1]. Contralateral C7 (CC7) transfer has been used for treating traumatic BPI, but the efficacy of CC7 transfer causes heated debate in the society [4]. Only the combination of nerve repair with muscle and tendon transfer using both conventional and new methods, including the free muscle transplant innervated through vascularized nerve grafts, can make the patient use paralyzed arm functionally [5]. The BPI can be repaired using end-to-side side-to-side grafting neuroorrhaphy in root ruptures, in phrenic and spinal accessory nerve neurotization, in CC7 neurotization, and in neurotization using intact interplexus roots or cords [6].

Phrenic nerve injury is recognized as a complication following cardiac intervention or surgery, and with the common use of transcatheter procedures for treating drug-refractory arrhythmias, clarification of the spatial correlations between the phrenic nerves and significant cardiac structures is very necessary to reduce the risks of phrenic nerve injury [7]. End-to-side (ETS) vascular anastomosis has a pretty complexity regarding the suturing of the juncture line between the artery and the graft, and a stress-concentration method was put forward for predicting the stress distribution at the juncture line, aiming to offer generic expressions describing the response of an end-to-side anastomosis (ETSA) [8]. Although an intervention strategy targeting the extensors of the affected upper limb might be good for functional recovery, conventional repetitive motor training has restricted clinical utility; a recent study demonstrated that repetitive transcranial magnetic stimulation could induce motor recovery [9]. However, the effects of end-to-side screw anastomosis (ETSSA) of phrenic nerve on the recovery of limb function after BPI have not yet been reported. Thus, in our study, we made an *in vivo* study to investigate whether the ETSSA can effectively promote the recovery of motor function in rats with BPI.

Material and Methods

Ethics statement

This study was approved by the Animal Ethics Committee of Jinan Military General Hospital. All experimental animals

were used and killed strictly according to relevant laws and regulations.

Experimental animals and grouping

Ninety clean male Sprague-Dawley rats with the weight of 200 to 250 g, purchased from Better Biotechnology Co., Ltd. (Nanjing, China), were used in this study. Rats were randomly grouped into 3 groups, with 30 rats in each group. The left side of the rat was selected as the experimental side (affected side), and the right side was selected as the control side (unaffected side). The ETSA group had left brachial plexus root avulsion + nerve transplantation + ETSA of phrenic nerve displaced to the musculocutaneous nerve; the ETSSA group had left brachial plexus root avulsion + nerve transplantation + ETSSA for phrenic nerve displaced to the musculocutaneous nerve; the model group had left brachial plexus root avulsion without repair.

Establishment of rat models of BPI

The rats were anesthetized intraperitoneally with 5% ketamine (300 to 350 mg/kg) and fixed on the plate in the supine position with unfolding the limbs. After unhairing, 75% ethanol was used for routine disinfection of rats, the towel was spread on the plate, and the models were established under a 10 times operation microscope. An incision was made in the middle of the left upper limb and neck, and the skin was incised from the middle of the neck along the medial upper limb to the elbow. From the clearance between the pectoralis major muscle and biceps brachii muscle, a pull hook was used to pull a part of the pectoralis major to the opposite side to expose the brachial plexus in the upper limb, in which the musculocutaneous nerve was dissected and marked for following use. In the neck incision, the clavicle was pulled to the opposite side using a clavicular hook to reveal the left C5–T1 nerves (Figure 1A). Then the C5–T1 nerves root were completely cut off successively to simulate the pathological state of left total brachial plexus root avulsion (Figure 1B). The musculocutaneous nerve was cut at 0.5 cm from biceps brachii muscle in the incision of upper arm. Subsequently, 2.0 cm of the saphenous nerve (SN) of the ipsilateral lower limb was obtained as the transplanted nerve bridging the muscle cutaneous nerve and the phrenic nerve. All sutures were sutured with 12-0 non-invasive nylon thread without tension. For the ETSA group, the distal end of SN and the musculocutaneous nerve were anastomosed with an end-to-end anastomosis, and 2 stitches were sutured; the proximal end of SN and the phrenic nerve was anastomosed with a 45° end-to-end anastomosis to the phrenic nerve trunk, and 1 stitch was sutured. For the ETSSA group, the distal end of SN and the musculocutaneous nerve were anastomosed with an end-to-end anastomosis, and 2 stitches were sutured (Figure 1C); the proximal end of SN spirally

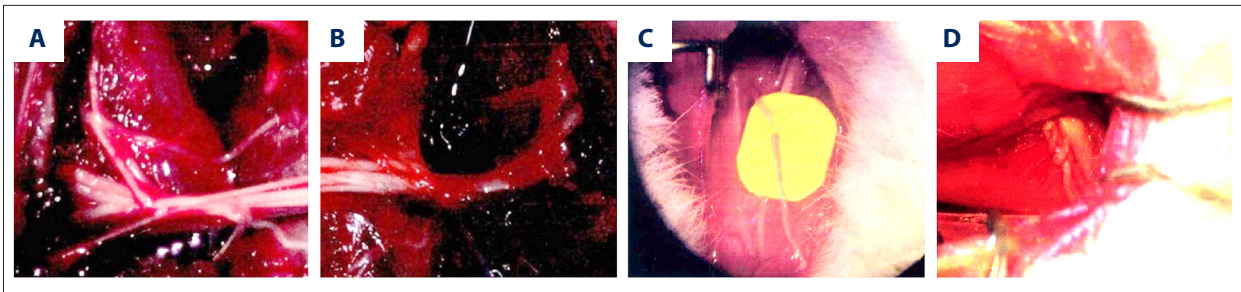


Figure 1. Surgical treatment of rats in model establishment of BPI. (A) The intact brachial plexus in normal rats; (B) the total brachial plexus root avulsion; (C) the end-to-end anastomosis of SN with the musculocutaneous nerve; (D) the end-to-side anastomosis of SN with the phrenic nerve after SN spirally twisted the phrenic nerve; BPI – brachial plexus injury; SN – saphenous nerve.

twisted the phrenic nerve in 3.5 cycles with a 45° ETSA to the phrenic nerve trunk, and each spiral was sutured with 1 stitch (Figure 1D). For the model group, all the nerve-end back packs were folded into the adjacent muscle tissue without any repair. After the operation, local irrigation with normal saline was performed, and penicillin sodium powder was placed in the incision to prevent infection. After suturing with 5-0 silk threads, the rats were fed routinely.

Behavioral observation

The time of elbow flexion synchronizing with breathing was observed on the affected side of 10 rats in each group at 1 and 3 months after operation, respectively. Behavioral observation was performed using the Terzis grooming test [10]. Then 3 mL water was sprayed into the nose of rats by using a syringe, and the action of cleaning the nasal water droplets in the rats was observed and classified into 0–5 grades: rats without any reaction as 0; rats that can elbow but cannot touch the nose as 1; rats that can elbow and touch the nose as 2; rats that can elbow to the position below the eyes as 3; rats that can elbow to the eye as 4; rats that can elbow to the ear or the back position of ears as 5.

Electoneurophysiological examination

The compound muscle action potential (CMAP) of biceps brachii muscle of 10 rats in each group on the affected side and unaffected side was detected using Dantec-Neuromatic 2000 (Dantec, Skovlund, Denmark) at 1 and 3 months after operation. The intensity of stimulation current was the minimum stimulus that causes the maximum amplitude, and the wave width was 0.04 ms. The latent period and amplitude of CMAP of biceps brachii on the affected and unaffected side were recorded, and then the latency delayed rate (LDR) and amplitude recovery rate (ARR) were calculated. The formulas were: $LDR = \text{affected latency} / \text{unaffected latency}$, $ARR = \text{affected amplitude} / \text{unaffected amplitude}$.

Muscular tension recovery rate (MTRR) measurement

Muscle tension on the affected side and unaffected side of rats in each group was detected using physiological experiment multi-purpose instrument (Shanghai Yilian Latrical Instrument Equipment Co., Ltd., Shanghai, China) at 1 and 3 months after operation. The biceps brachii muscles of rats on both sides were cut off at the point of radial tuberosity, and then connected to the muscular tension transducer after suturing with 1/10 silk suture. The biceps brachii muscle was controlled at the initial length by adjusting the traction tension. The parameters of the software were set as: electric stimulation intensity=8 V, frequency=15 Hz, wave width=3 ms, sensitivity=24 g, string pulse number=15, series pulse interval=70 ms, sampling interval=2 ms, single sampling. The musculocutaneous nerves were stimulated by electrode 1 cm away from the entry point of the musculocutaneous nerve. The tetanic contraction curve of biceps brachii was recorded, and the tetanic tension on both sides was measured. The muscle was always kept moist during the determination. $MTRR = \text{tetanic tension on the affected side} / \text{tetanic tension on the unaffected side}$.

Hematoxylin and eosin (H&E) staining and determination of muscle weight recovery rate (MWRR) and cross-sectional area recovery rate (CARR) of muscle cells

The biceps brachii on the affected side and unaffected side was dissected completely from rats in each group at 1 and 3 months after operation. The surface connective tissues were removed and immediately weighed and analyzed by analytical balance (R200D, 1/100000, Germany). After the measurement of muscle wet weight, the muscle specimens were placed in 8% formaldehyde solution to fix for 72 hours. After dehydration by gradient alcohol and paraffin embedding, the muscle specimens were sliced into 5- μm sections by automatic slicing machine (Reichert-Jung 2050) and then stained by H&E. Leica DWLB2 microscope (Leica, Germany) was used to observe 5 horizons randomly (400 \times). Leica-Qwin image analysis software (Leica, Germany) was used to measure the total

number of muscle cells and the total cross-sectional area in the selected views, thereby calculating the average value of cross-sectional area of each muscle cell. The MWRR and CARR of the muscle cells were calculated using the following formulas: MWRR=muscle wet weight of the affected side/muscle wet weight of the unaffected side; CARR=cross-sectional area of muscle cells on the affected side/cross-sectional area of muscle cells on the unaffected side.

Counting of regenerated myelinated nerve fibers

The repairing segmental nerves formed after suturing were removed from rats in each group at 1 and 3 months after operation. Then 2 mm of proximal phrenic nerve and 2 mm of distal musculocutaneous nerve were obtained and fixed with 0.25% glutaraldehyde for 72 hours. After the specimens were dehydrated by gradient alcohol and embedded by epoxy resin, they were cut into 0.5 μ m of ultra-thin sections which were stained with 5% toluidine blue, separated by 20% acetic acid, washed several times by water, dried and sealed. Leica DWLB2 microscope (Leica, Germany) was used to observe 5 horizons randomly (400 \times). Leica-Qwin image analysis software (Leica, Germany) was used to count the area of visual field (A), in which the number of myelinated nerve fibers was counted, and the average value (N) of myelinated nerve fibers number in 5 fields was calculated. The average density of myelinated nerve fibers $\rho=N/A$, and total number of myelinated nerve fibers $TN=\rho\times TA$ (TA is the total cross-sectional area of the nerve). The numbers of myelinated nerve fibers of rats in each group in the proximal phrenic nerve and distal musculocutaneous nerve of suture were counted, and the regenerated nerve traversing rate (NTR) was calculated. $NTR=\text{the number of distal myelinated nerve fibers}/\text{the number of proximal myelinated nerve fibers}$.

Motor endplate examination

The frozen sections of the biceps brachii on the affected side and the unaffected side of rats in each group were cut at 1 and 3 months after operation, and then dried for 30 min at room temperature. Kamovsky-Roots solution (100 μ L of 0.1 mol/L sodium citrate, 200 μ L of 30.0 mmo/L copper sulfate, 200 L of distilled water, 200 μ L of 5 mmo/L sodium ferricyanide and 1.0 mg of sulfide acetylcholine were added into 1.3 mL of 0.1 mol/L acetate buffer successively) was added into the frozen sections, which were incubated at 37°C for 30 to 40 min, counterstained with hematoxylin for 5 min and sealed with gum. BI-2000 image analyzer (Chengdu Techman Software Co., Ltd., Chengdu, China) was used to determine the area of motor endplate.

Statistical analysis

All data were processed by SPSS 21.0 software (IBM Corp. Armonk, NY, USA). The measurement data were expressed

Table 1. Grading of Terzis grooming test in rats of the ETSA, ETSSA and model groups (mean \pm SD, grade).

Group	1 month after operation	3 months after operation
ETSA group	1.51 \pm 0.32	3.21 \pm 0.21*#
ETSSA group	1.58 \pm 0.24	3.30 \pm 0.36*#
Model group	0	0

* $P<0.05$ compared with 1 month after operation; ETSSA – end-to-side screw anastomosis; ETSA – end-to-side anastomosis; SD – standard deviation.

as mean \pm standard deviation (SD). Comparison between 2 groups was tested by independent sample *t*-test, and comparison among multiple groups was analyzed by one-way analysis of variance (ANOVA). Comparison of parameters at different time points in the same group was done using repeated measures ANOVA. $P<0.05$ was considered statistically significant.

Results

The grading of Terzis grooming test in the ETSA and ETSSA groups increased with time

At 1 and 3 months after operation, muscle atrophy occurred on the affected side of rats in the model group, and there was no elbow flexion movement induced by respiratory motion. The grading of Terzis grooming test was 0. At 1 month after the operation, 3 rats in both the ETSA group and the ETSSA group produced minor elbow flexion movement on the left side of body. At 3 months after operation, 9 rats in the ETSA group produced elbow flexion movement, while elbow flexion movement could be observed from all rats in the ETSSA group. But there was no significant difference between the 2 groups ($P>0.05$). The range of elbow flexion movement in the ETSA and ETSSA groups at 3 months after operation was higher than those at 1 month after operation. At 1 and 3 months after operation, the grading of Terzis grooming test in the ETSA and ETSSA groups increased with time (all $P<0.05$), and there was no significant difference between the 2 groups (all $P>0.05$) (Table 1).

BPI rats treated with ETSSA showed lower LDR of CMAP but higher ARR of CMAP

At 1 and 3 months after operation, the latent period and maximum amplitude of CMAP of biceps brachii on both sides of rats in each group are shown in Table 2. The model group had no CMAP. After operation, the latent period of CAMP of biceps brachii on the affected side of rats in each group shortened gradually (all $P<0.05$), but the maximum amplitude increased

Table 2. The latent period and maximum amplitude of CMAP of biceps brachii on both sides of rats in the ETSA, ETSSA and model groups at 1 and 3 months after operation (mean \pm SD).

Group	1 month after operation		3 months after operation	
	Affected side	Unaffected side	Affected side	Unaffected side
ETSA group	4.28 \pm 0.43	1.31 \pm 0.24	2.17 \pm 0.27**	1.33 \pm 0.18
ETSSA group	4.01 \pm 0.38	1.31 \pm 0.20	1.54 \pm 0.19**	1.33 \pm 0.21
Model group	0	1.33 \pm 0.21	0	1.32 \pm 0.23
ETSA group	8.39 \pm 0.62	18.26 \pm 3.17	13.55 \pm 1.02**	18.13 \pm 3.05
ETSSA group	9.19 \pm 0.27	18.13 \pm 3.28	17.00 \pm 1.29**	18.42 \pm 2.84
Model group	0	18.19 \pm 3.31	0	18.24 \pm 3.25

* $P < 0.05$ compared with 1 month after operation; ETSSA – end-to-side screw anastomosis; ETSA – end-to-side anastomosis; CMAP – compound muscle action potential.

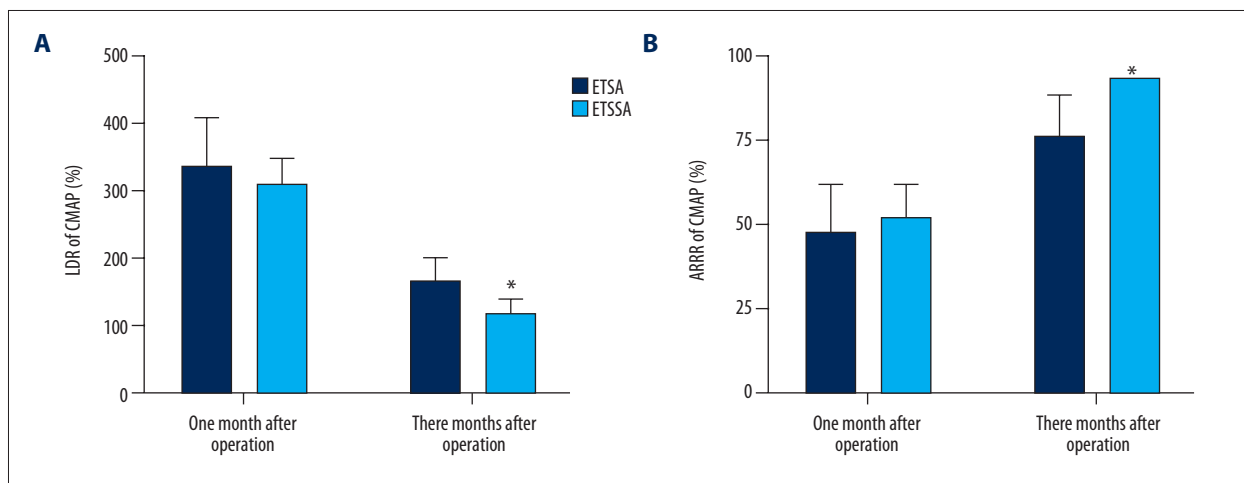


Figure 2. The LDR and the ARR of CMAP of biceps brachii of rats in the ETSA and ETSSA groups at 1, 2, and 3 months after operation. * $P < 0.05$ compared with the ETSA group; LDR – latency delayed rate; ARR – amplitude recovery rate; ETSSA – end-to-side screw anastomosis; ETSA – end-to-side anastomosis.

gradually ($P < 0.05$). At 1 month after operation, there was no significant difference in the LDR and the maximum ARR between the ETSA and ETSSA groups (all $P > 0.05$). At 3 months after operation, the LDR and the maximum ARR of CMAP of rats in the ETSSA group were 118.48% and 93.19%, respectively. The LDR of CMAP in the ETSSA group was lower than that in the ETSA group, but the ARR of CMAP in the ETSSA group was higher than that in the ETSA group (all $P < 0.05$) (Figure 2).

BPI rats treated with ETSSA displayed better MTRR of biceps brachii

At 1 and 3 months after operation, the biceps brachii on the affected side of rats in the ETSA and ETSSA groups reacted to electrical stimulation, while the muscular tension of biceps brachii on the affected side of rats in the model group was not detected. At 1 and 3 months after operation, the MTRR of biceps brachii on the affected side of rats in the ETSA and ETSSA groups

increased with time. There was no statistical significance for comparing the differences between the 2 groups at 1 month after operation ($P > 0.05$). At 3 months after operation, the MTRR of rats in the ETSSA group was 71.95%, which was significantly higher than that in the ETSA group ($P < 0.05$) (Figure 3). The tetanic tension of biceps brachii on the affected side of rats in the ETSSA group nearly recovered to the preoperative level.

BPI rats treated with ETSSA presented with better recovered muscle cell morphology

At 1 month after operation, compared with the unaffected side, necrosis, disintegration and lymphocytic infiltration, and decreased cell size appeared in biceps muscle cells on the affected side of rats in each group. The model group was particularly serious, followed by the ETSA group and the ETSSA group. With the increase of time, the morphology of muscle cells in the ETSA and ETSSA groups gradually recovered and was close to

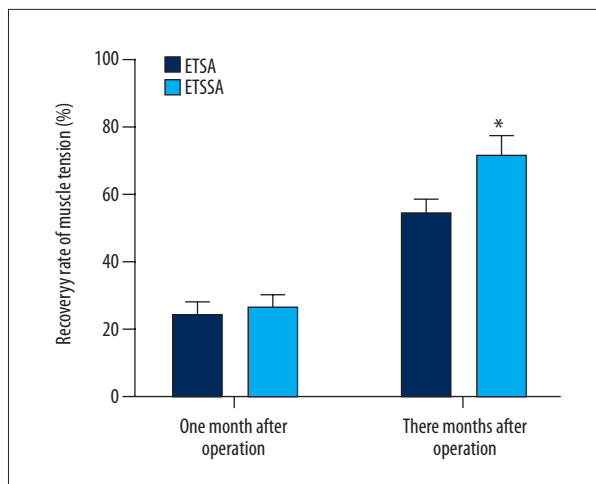


Figure 3. The MTRR of biceps brachii on the affected side of rats in the ETSA and ETSSA groups at 1, 2, and 3 months after operation. * $P < 0.05$ compared with the ETSA group; MTRR – muscular tension recovery rate; ETSSA – end-to-side screw anastomosis; ETSA – end-to-side anastomosis.

those on the unaffected side. But the extent of cell morphology decrease in the model group was not relieved. The connective tissue between the muscle cells in the model group was significantly higher than that in the ETSA and ETSSA groups (Figure 4).

BPI rats treated with ETSSA exhibited elevated MWRR on the affected side

At 1 and 3 months after operation, the muscle wet weight of rats in the model group was slightly reduced, and the MWRR

was significantly lower compared with the ETSA and ETSSA groups (all $P < 0.05$). The muscle wet weight of biceps brachii on the affected side of rats in the ETSA and ETSSA groups recovered gradually with the passage of time. At 3 months after operation, the MWRR on the affected side in the ETSA and ETSSA groups were 64.62% and 71.97% respectively, and the MWRR in the ETSSA group was significantly higher than that in the ETSA group ($P < 0.05$) (Figure 5A). At 1 and 3 months after operation, the CARR of muscle cells in the model group was significantly lower than those in the ETSA and ETSSA groups (all $P < 0.05$). There was no significant difference between the ETSA and ETSSA groups ($P > 0.05$) (Figure 5B).

BPI rats treated with ETSSA revealed better postoperative regeneration of myelinated nerve fiber

After operation, the number of regenerated myelinated nerve fibers in the ETSA and ETSSA groups increased gradually with time, but the regenerated myelinated nerve fibers were not observed in the model group (Table 3). At 1 month after operation, the biceps brachii on the affected side of rats in the ETSA and ETSSA groups produced a large amount of nerve growth factor, which induced the lateral branches of phrenic nerve to produce relative small new nerve fibers. There was no significant difference in the number of regenerated myelinated nerve fibers and the NTR between the ETSA and ETSSA groups (all $P > 0.05$). At 3 months after operation, the thick nerve fibers in fresh myelinated nerve fibers in the ETSA and ETSSA groups gradually increased, and the number of regenerated myelinated nerve fibers and the NTR in the ETSSA group was significantly higher than those in the ETSA group (all $P < 0.05$). The results indicated that the postoperative regeneration of

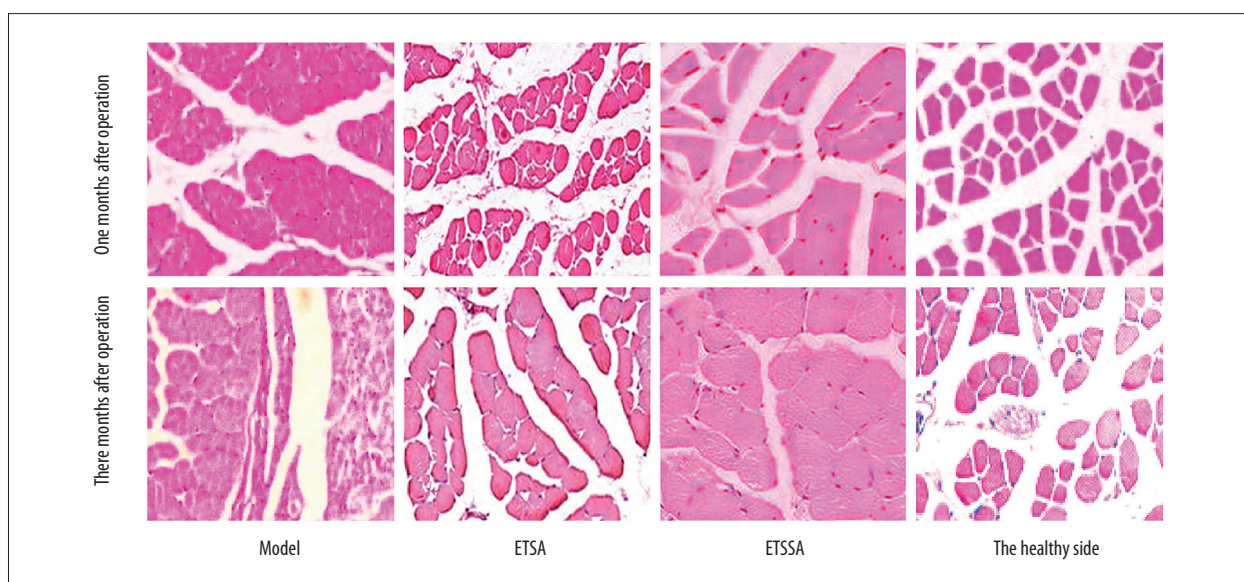


Figure 4. H&E staining of biceps brachii of rats in the ETSA, ETSSA and model groups at 1, 2, and 3 months after operation (200×). H&E – hematoxylin-eosin; ETSSA – end-to-side screw anastomosis; ETSA – end-to-side anastomosis.

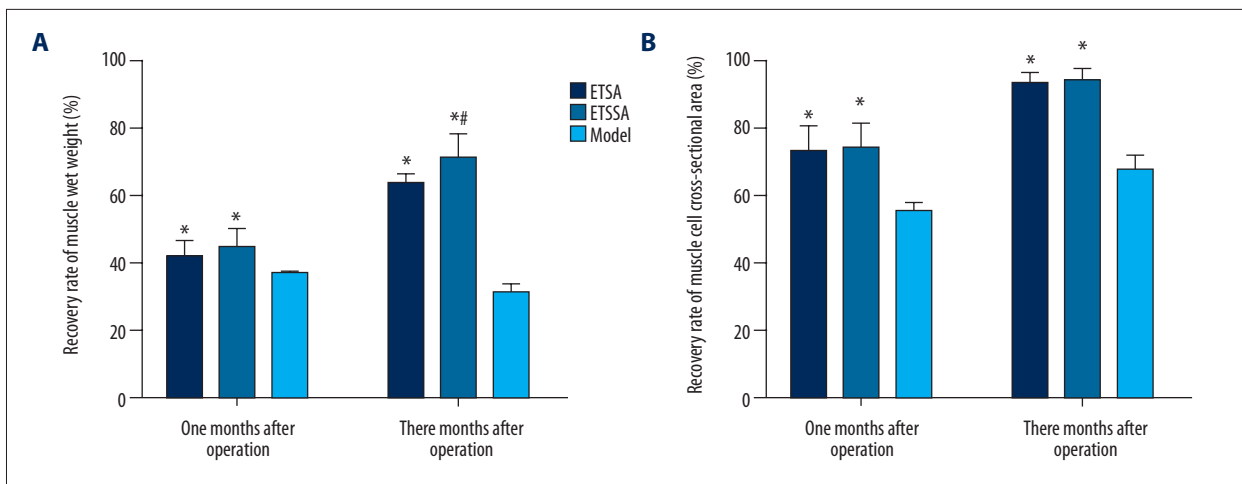


Figure 5. The MWRR and CARR of muscle cells of rats in the ETSA, ETSSA, and model groups at 1, 2, and 3 months after operation. (A) The MWRR of muscle cells of rats in three groups at 1, 2, and 3 months after operation; (B) the CARR of muscle cells of rats in three groups at 1, 2, and 3 months after operation. * $P < 0.05$ compared with the model group; # $P < 0.05$ compared with the ETSA group; MWRR – muscle weight recovery rate; CARR – cross-sectional area recovery rate; ETSSA – end-to-side screw anastomosis; ETSA – end-to-side anastomosis.

Table 3. The number of regenerated myelinated nerve fibers of rats in the ETSA, ETSSA and model groups at 1 and 3 months after operation (mean \pm SD).

Group	1 month after operation	3 months after operation
ETSA group	138.11 \pm 25.37	1223.70 \pm 77.37
ETSSA group	141.85 \pm 21.82	1467.77 \pm 67.57*
Model group	0	0

* $P < 0.05$ compared with the ETSA group; ETSSA – end-to-side screw anastomosis; ETSA – end-to-side anastomosis.

myelinated nerve fibers in the ETSSA group was better than that in the ETSA group (Figure 6).

BPI rats treated with ETSSA showed increased motor endplate

At 1 and 3 months after operation, the motor endplate on the affected side of rats in the ETSA and ETSSA groups had large area, clear structure and was deeply colored, while the motor endplate on the affected side of rats in the model group had small area, obscure structure and was lightly colored. Compared with the model group, the area of motor endplate in the ETSA and ETSSA groups were significantly higher ($P < 0.05$), and the motor endplate area in the ETSSA group was significantly higher than that in the ETSA group ($P < 0.05$), as shown in Table 4.

Discussion

In this study, we explored the effect of ETSSA of phrenic nerve on the recovery of limb function after BPI. The results showed that ETSSA had better efficacy, for the reason that it is able to restore the limb function recovery to a greater extent and accelerate the regeneration of nerve fibers in rats with BPI.

According to our study results, the grading of Terzis grooming test in the ETSSA and ETSA groups increased with time at 1 and 3 months after operation. ETS neurotomy is a technology that can address the problem of distal target reinnervation without injury to the original donor nerve, and the technique drew wide attention after Viterbo reported his experiments in 1992 [11]. As a possible therapy for treating nerve lesions without practicable proximal nerve stumps, ETS neurotomy has been practicably and clinically researched [12]. Moreover, ETS neurotomy, also lateral anastomosis, has been confirmed to be an alternative way to reconstruct severed peripheral nerves [13]. The Terzis grooming test that evaluates and describes actions and behaviors is a useful test applied to the neural system, reflecting the reconstruction and maturation of the target muscle motor units after nerve reinnervation [14,15]. The functional recovery of biceps brachii is reflected by improved behaviors in rats, such as elbow flexion lifting, or shoulder abduction [16]. Therefore, the results in the present study showed the well recovery of muscle function, implying that ETSA and ETSSA for phrenic nerve could promote the recovery of motor function in rats

Additionally, the decreased LDR and increased maximum ARR of CMAP, MWRR, and MTRR of rats in the ETSA group, and ETSSA groups compared with the model group, indicated that ETSA

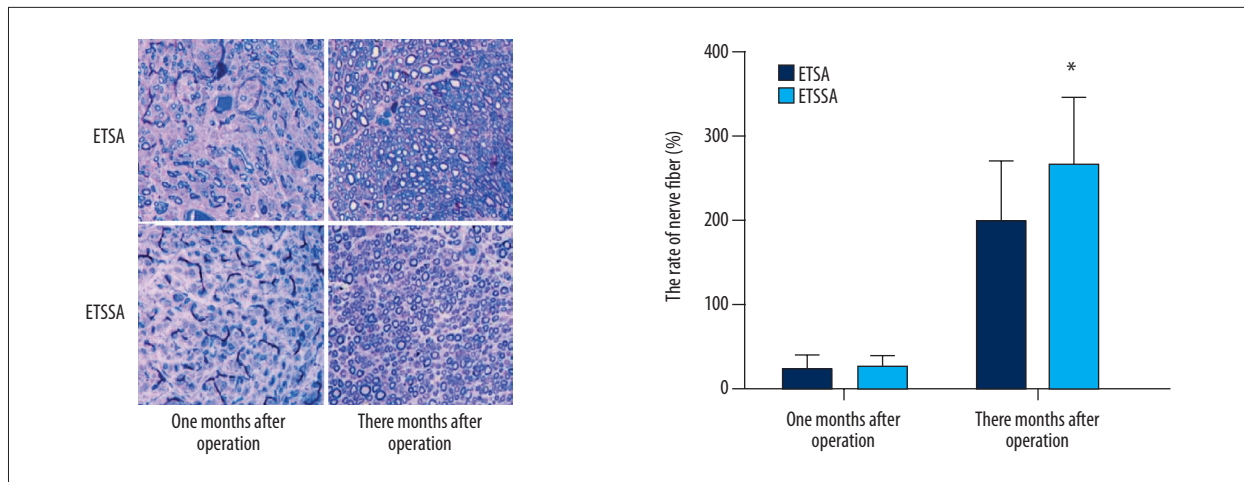


Figure 6. Toluidine blue staining of myelinated fibers in the distal end of musculocutaneous nerve (400×) and the NTR. * $P < 0.05$ compared with the ETSA group; NTR – nerve traversing rate; ETSA – end-to-side anastomosis.

Table 4. Motor endplate area of rats in the ETSA, ETSSA and model groups at 1 and 3 months after operation (mean \pm SD).

Group	1 month after operation	3 months after operation
ETSA group	252.75 \pm 36.53*	251.31 \pm 34.96*
ETSSA group	295.67 \pm 35.54**	296.97 \pm 35.15**
Model group	215.12 \pm 28.61	153.29 \pm 14.25

* $P < 0.05$ compared with the model group; ETSSA – end-to-side screw anastomosis; ETSA – end-to-side anastomosis.

and ETSSA for phrenic nerve could shorten the latent period and increase the maximum amplitude of CMAP, and then promote the recovery of biceps brachii muscle, but the efficacy of ETSSA was better compared with that of ETSA. The CMAP onset latency reflects the arrival time at the impulse muscle in the fastest-conducting motor nerve fiber [17]. Liao et al. demonstrated that both ETS and end-to-end neurorrhaphy can restore the function of recipient nerves as well as maintain the normal function of donor nerves, and better efficacy is related to higher amplitude of CMAP and shorter latency and density of motor end plates [18], which was consistent with our data. Additionally, Liu et al. reported that ETS neurorrhaphy promoted effective motor functional recovery, which was characterized by higher density of regenerated axons, greater muscle weight, stronger muscle contractile function, and primitive improvement of the peroneal functional index in comparison to unrepaired nerves [19], which further supported our results.

Furthermore, the number of regenerated myelinated nerve fibers, NTR, and the motor endplate area of rats in the ETSSA and ETSA groups were higher than those in the model group,

from which we can hypothesize that ETSSA could promote limb function recovery. Motor endplates, whose location is not known in the majority of muscles, is the key site for botulinum neurotoxin action that decreases the contraction of disabling muscles [20]. It has been found that peripheral nerve axons regenerating at the injury site at a speed of nearly 1 mm/d can contribute to muscle reinnervation by interacting with their target motor endplates [21]. By comparing the sural nerve biopsies of diabetic patients with damaged glucose tolerance and those with normal glucose tolerance, a strong association was found between a decreased density of myelinated nerve fibers, abnormal electrophysiological function and neuropathic clinical signs [22]. What's more, low myelinated nerve fiber density was demonstrated to be correlated with nerve dysfunction progression as well [23,24]. From those data, we can conclude that the results in the present study suggest a gradual recovery of limb function in brachial plexus.

Conclusions

Our study provided evidence that ETSSA is capable of restoring limb function recovery to a greater extent, and accelerating the regeneration of nerve fibers in rats with BPI, with a better effect in the ETSSA group compared with the ETSA group. The data implied that ETSSA for phrenic nerve is expected to be a potential treatment for BPI. Restricted by the number of samples, however, the experimental results are not fully representative. Because of the fact that the diameters of nerves and muscles which may be neurotized in human are much bigger and not comparable with rats, it is advised to conduct experiments based on animals with bigger nerves and muscles size, such as primates, to increase authenticity and reliability. What's more, there was no comparison of the therapeutic effect of ETSSA and ETSA in this study. Therefore, further research is needed to confirm our conclusions.

Conflicts of interests

None.

References:

1. Yoshikawa T, Hayashi N, Yamamoto S et al: Brachial plexus injury: Clinical manifestations, conventional imaging findings, and the latest imaging techniques. *Radiographics*, 2006; 26(Suppl. 1): S133-43
2. Doumouchtsis S K, Arulkumaran S: Are all brachial plexus injuries caused by shoulder dystocia? *Obstet Gynecol Surv*, 2009; 64: 615-23
3. Volpe K A, Snowden J M, Cheng Y W et al: Risk factors for brachial plexus injury in a large cohort with shoulder dystocia. *Arch Gynecol Obstet*, 2016; 294: 925-29
4. Yang G, Chang KW, Chung KC: A systematic review of outcomes of contralateral C7 transfer for the treatment of traumatic brachial plexus injury: Part 2. Donor-site morbidity. *Plast Reconstr Surg*, 2015; 136: 480e-89e
5. Berger A, Schaller E, Mailander P: Brachial plexus injuries: an integrated treatment concept. *Ann Plast Surg*, 1991; 26: 70-76
6. Amr SM, Moharram AN: Repair of brachial plexus lesions by end-to-side side-to-side grafting neurotaphy: Experience based on 11 cases. *Microsurgery*, 2005; 25: 126-46
7. Sanchez-Quintana D, Cabrera J A, Climent V et al: How close are the phrenic nerves to cardiac structures? Implications for cardiac interventionalists. *J Cardiovasc Electrophysiol*, 2005; 16: 309-13
8. Roussis PC, Giannakopoulos AE, Charalambous HP: Suture line response of end-to-side anastomosis: A stress concentration methodology. *Cardiovasc Eng Technol*, 2015; 6: 36-48
9. Koganemaru S, Mima T, Thabit MN et al: Recovery of upper-limb function due to enhanced use-dependent plasticity in chronic stroke patients. *Brain*, 2010; 133: 3373-84
10. Inciong JG, Marrocco WC, Terzis JK: Efficacy of intervention strategies in a brachial plexus global avulsion model in the rat. *Plast Reconstr Surg*, 2000; 105: 2059-71
11. Noah EM, Williams A, Fortes W et al: A new animal model to investigate axonal sprouting after end-to-side neurotaphy. *J Reconstr Microsurg*, 1997; 13: 317-25
12. Zhang F, Fischer KA: End-to-side neurotaphy. *Microsurgery*, 2002; 22: 122-27
13. Dubovy P, Raska O, Klusakova I et al: Ciliary neurotrophic factor promotes motor reinnervation of the musculocutaneous nerve in an experimental model of end-to-side neurotaphy. *BMC Neurosci*, 2011; 12: 58
14. Reidinger RF Jr, Mason JR: Effects of learned flavor avoidance on grooming behavior in rats. *Physiol Behav*, 1986; 37: 925-31
15. Bastedo L, Sands MS, Lambert DT et al: Behavioral consequences of bone marrow transplantation in the treatment of murine mucopolysaccharidosis type VII. *J Clin Invest*, 1994; 94: 1180-86
16. Zou L, Cao X, Li J et al: Improved C3-4 transfer for treatment of root avulsion of the brachial plexus upper trunk: Animal experiments and clinical application. *Neural Regen Res*, 2012; 7: 1545-55
17. Phongsamart G, Wertsch JJ, Ferdjallah M et al: Effect of reference electrode position on the compound muscle action potential (CMAP) onset latency. *Muscle Nerve*, 2002; 25: 816-21
18. Liao WC, Chen JR, Wang YJ et al: The efficacy of end-to-end and end-to-side nerve repair (neurotaphy) in the rat brachial plexus. *J Anat*, 2009; 215: 506-21
19. Liu K, Chen LE, Seaber AV et al: Motor functional and morphological findings following end-to-side neurotaphy in the rat model. *J Orthop Res*, 1999; 17: 293-300
20. Amirali A, Mu L, Gracies J M et al: Anatomical localization of motor end-plate bands in the human biceps brachii. *J Clin Neuromuscul Dis*, 2007; 9: 306-12
21. Menashe SJ, Tse R, Nixon JN et al: Brachial plexus birth palsy: Multimodality imaging of spine and shoulder abnormalities in children. *Am J Roentgenol*, 2015; 204: W199-206
22. Dahlin LB, Sanden H, Dahlin E et al: Low myelinated nerve-fibre density may lead to symptoms associated with nerve entrapment in vibration-induced neuropathy. *J Occup Med Toxicol*, 2014; 9: 7
23. Eriksson K F, Nilsson H, Lindgarde F et al: Diabetes mellitus but not impaired glucose tolerance is associated with dysfunction in peripheral nerves. *Diabet Med*, 1994; 11: 279-85
24. Sundkvist G, Dahlin LB, Nilsson H et al: Sorbitol and myo-inositol levels and morphology of sural nerve in relation to peripheral nerve function and clinical neuropathy in men with diabetic, impaired, and normal glucose tolerance. *Diabet Med*, 2000; 17: 259-68